A Semi-Empirical Determination of the Shape of Cloud and Rain Drops

H. R. PRUPPACHER AND R. L. PITTER

Dept. of Meteorology, University of California, Los Angeles

(Manuscript received 29 June 1970)

ABSTRACT

A physical model which predicts the shape of water drops falling at terminal velocity in air is presented. The model is based on a balance of the forces which act on a drop falling under gravity in a viscous medium. The model was evaluated by numerical techniques and the shape of water drops of radii between 170 and 4000 μ (equivalent to Reynolds numbers between 30 and 4900) was determined. The results of our investigation show that the drop shapes predicted by the model agree well with those experimentally observed in our wind tunnel. Both theory and experiment demonstrate that: 1) drops with radii $\lesssim 170\,\mu$ are very slightly deformed and can be considered spherical, 2) the shape of drops between about 170 and 500 μ can be closely approximated by an oblate spheroid, 3) drops between about 500 and 2000 μ are deformed into an asymmetric oblate spheroid with an increasingly pronounced flat base, and 4) drops $\gtrsim 2000\,\mu$ develop a concave depression in the base which is more pronounced for larger drop sizes. The relevance of these findings to the process of drop breakup is discussed.

1. Introduction

It is well known from observation that water drops falling at terminal velocity in air are hydrodynamically unstable and break up if they are larger than a certain critical size. In a fundamental paper, Langmuir (1948) pointed out that this decisively influences the rate of formation of precipitation within clouds. When a drop growing by collision and coalescence becomes unstable and breaks up, each fragment drop is capable of growing by collision and coalescence until it, too, breaks up. In such clouds the growth of precipitation proceeds in an "avalanche-like" manner. Experiments reported in the literature have established that the drop shape, which is dependent upon the drop size, is the determining variable for the hydrodynamic stability of a water drop in air.

In a recent paper Pruppacher and Beard (1970) reviewed previously published work on the shape of water drops falling in air. They showed that the results of previous experimental investigations (Lenard, 1904; Blanchard, 1948, 1950, 1955; Garner and Lane, 1959; Best, 1947; Jones, 1959; Kumai and Itagaki, 1954; Magono, 1954) scatter greatly due to numerous experimental difficulties. Present available theoretical and semi-empirical attempts to predict the drop shape as a function of size have also failed to produce exact results. The theoretical attempts either disregarded viscous effects (Imai, 1950), were based on an incomplete balance of forces acting on the drop (Spilhaus, 1948; Savic, 1953), or were applicable only to very small Reynolds numbers (Taylor and Acrivos, 1964). New experimental results on the shape of water drops in air were presented by Pruppacher and Beard. Their results were obtained from photographs of drops freely suspended in the air stream of a large, vertical wind tunnel. In the present paper, we attempt to confirm these recent results on the basis of theoretical considerations.

2. Formulation of the model

Some time ago Savic (1953) outlined a semi-empirical method for determining the deformation of a drop falling under gravity in a viscous medium. His method was based on a balance of forces which act on a falling drop. These include the aerodynamic pressure due to fluid flow past the falling drop, the hydrostatic pressure gradient inside the drop, and the pressure increment across the drop surface of given curvature and surface tension. Our analysis revealed that, apart from a considerable number of serious typographical errors in the equations presented in his report, Savic's theory and calculations suffer from a number of deficiencies:

1) His pressure balance equation is in error by a constant pressure term which, even though unimportant for determining the drop shape, is essential for a quantitatively correct pressure balance around the drop.

2) The effects of the hydrostatic pressure gradient inside the drop were only approximately taken into account.

3) Savic assumed that the aerodynamic pressure around a falling drop can be estimated from the pressure distribution around a sphere. He thus assumed that all the forces considered for balance are unaffected by the drop deformation. No justification for this assumption was given even though it is known from experiment and theory that the pressure distribution around a body

submerged in a moving fluid is a function of the shape of that body as well as of the physical characteristics of the fluid.

4) For numerical evaluation of his model, Savic used the pressure distribution around a rigid sphere determined experimentally by Flachsbart (1927). However, more accurate measurements are available.

5) Flachsbart's pressure measurements are only applicable to Reynolds numbers between about 10^3 and 10^5, where the Reynolds number is defined by $N_{\mathrm{Re}}=2a_0V_\infty/\nu_a$, in which V_∞ is the free stream velocity, ν_a the kinematic viscosity of air and a_0 the equivalent radius, defined as the radius of a sphere with the same volume as the deformed drop. The deformation of drops with Reynolds numbers $<10^3$ could not be computed by Savic.

6) He neglected the presence of an internal circulation in a falling drop, and its effects on the drop shape. However, Garner and Lane (1959) and Pruppacher and Beard (1970) have shown that water drops falling in air have well-developed internal circulations.

We investigated each of these deficiencies in Savic's model and attempted to improve upon them in ours. The complete equation for the balance of forces around a drop can be found as follows. Using, as illustrated in Fig. 1, a polar coordinate system placed in a meridional plane through a drop and centered at the center of mass of the drop, the pressure balance for an arbitrary position on the surface of the drop can be written as

$$\sigma[1/R_1(\theta)+1/R_2(\theta)]=p_i(\theta)-p_e(\theta), \tag{1}$$

where θ is the polar angle from the forward stagnation point, p_i the internal pressure of the drop, p_e the aerodynamic pressure at the drop surface, R_1 and R_2 the principal radii of curvature of the drop surface, and σ the surface tension of water. For the internal pressure we can write

$$p_i(\theta)=p_i(\theta=\pi)+g(\rho_w-\rho_a)(r_0+r\cos\theta)+p_{ic}(\theta), \tag{2}$$

where

$$p_i(\theta=\pi)=p_e(\theta=\pi)+2\sigma/R(\theta=\pi), \tag{3}$$

p_{ic} is the contribution to the internal pressure due to internal circulation, ρ_w and ρ_a are the densities of water and air, g the acceleration of gravity, r the magnitude of the radius vector to a point on the drop surface, and $r_0=r(\theta=\pi)$. Adding and subtracting the static pressure p_∞, the pressure balance equation becomes

$$\sigma[1/R_1(\theta)+1/R_2(\theta)]=g(\rho_w-\rho_a)(r_0+r\cos\theta)-[p_e(\theta)-p_\infty]+p_{ic}(\theta)+[p_i(\theta=\pi)-p_\infty]. \tag{4}$$

The term on the left-hand side of this equation is the curvature term. The terms on the right-hand side, in order, represent the hydrostatic pressure inside the drop, the aerodynamic pressure at the surface of the drop, the contribution to the internal pressure due to internal circulation in the drop, and the internal pressure excess at the top of the drop. We shall now elaborate on each of these terms.

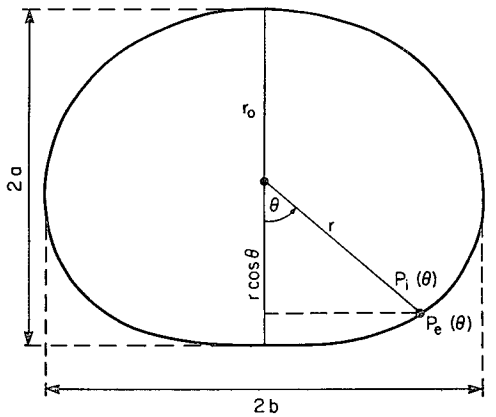

FIG. 1. Schematic illustration of the terminology used in text.

The last term on the right-hand side of (4) is a constant with respect to the angle θ. Consequently, this term does not contribute to the shape of the drop.

The hydrostatic pressure term can be evaluated by assuming that the deformation of the drop is small and that the terms describing the distortion of the drop only enter the calculations as first-order perturbations. For these conditions the drop surface can be represented by

$$r=a_0\left(1+\sum_{n=0}^{\infty}c_n\cos n\theta\right), \tag{5}$$

where c_n are the deformation coefficients. From (5)

$$r_0=a_0\left(1+\sum_{n=0}^{\infty}c_n\cos n\pi\right).$$

Following Imai (1950), Savic (1953) and Landau and Lifshitz (1959), the curvature term can be expressed by a cosine series involving the deformation coefficients in the form

$$\sigma[1/R_1(\theta)+1/R_2(\theta)]=(\sigma/a_0)\left[2+\sum_{n=0}^{\infty}(n^2-2)c_n\cos n\theta+\sum_{n=0}^{\infty}nc_n\sum_{m=1}^{m=n}\cos(n-2m)\theta\right]. \tag{6}$$

Despite considerable search we could find no report on experimental measurements of the pressure distribution, $p_e(\theta)-p_\infty$, around objects of raindrop shape. Eichelbrenner and Michel (1957) measured the pressure distribution around rigid spheroids at Reynolds numbers of the order of 10^6, but these high Reynolds numbers are not applicable to the problem at hand. The theoretical expressions derived for the pressure

distribution around a rigid spheroid by Maruhn (1940) and Batchelor (1967) are not applicable to our problem either because they are based on non-viscous flow. However, the pressure distribution around a rigid sphere is well known over a wide Reynolds number interval from theory and experiment. Measurements of the pressure distribution around a rigid sphere in air were made by Fage (1937). His results are applicable to Reynolds numbers between 10^5 and about 10^3. The most recent theoretical calculations of the pressure distribution around a rigid sphere are those of LeClair *et al.* (1970) which are applicable to $0.01 \leqslant N_{\mathrm{Re}} \leqslant 400$. An evaluation of the quantity $p_e(\theta)-p_\infty$ in Eq. (4) from pressure distributions around rigid spheres would, however, introduce errors which become more serious the larger the drop. Therefore, an evaluation of the aerodynamic pressure term in this manner was undesirable.

Wind tunnel studies by Garner and Lane (1959) and ourselves on drops of a_0 between $100\,\mu$ and 0.35 cm demonstrated that water drops falling in air exhibit a well-developed internal circulation with a maximum estimated speed of $V_i \approx 15$ cm sec^{-1} in a drop of $a_0 = 0.35$ cm. Foote (1969) deduced from theory that the internal circulation in a drop decreases the curvature in the vicinity of the waist of the drop and thus reduces the drop deformation. Assuming potential flow inside a drop of equivalent radius $a_0 = 0.35$ cm ($N_{\mathrm{Re}} = 840$, with $\nu_w = 0.01$ cm^2 sec^{-1}), he proposed that the dynamic pressure due to internal circulation can be found from the relation, $p_{ic}(\theta) = \frac{1}{2}\rho_w V_i^2$. The internal circulation and consequently the dynamic pressure p_{ic} is largest near the minimum aerodynamic pressure around the drop which is near 90° for small drops and near 70°–80° for large drops. Our comparison shows that the dynamic pressure due to internal circulation, for the case of a drop of $a_0 = 0.35$ cm, is $\sim 20\%$ of the hydrostatic pressure inside the drop, and $\sim 14\%$ of the curvature term. No comparison with the aerodynamic pressure can be made unless more is known about the pressure distribution around a drop.

Some information which is very pertinent to our problem can be obtained from an article by McDonald (1954). McDonald used pressure balance considerations to determine the pressure distribution around four falling drops whose shape was given by photographs of Magono (1954). McDonald neglected the internal circulation term in his pressure balance equation although internal circulations did exist in the drops studied by Magono. The quantity which McDonald deduced from Magono's photographs was therefore $[p_e(\theta)-p_\infty]-p_{ic}(\theta)$ and not $p_e(\theta)-p_\infty$, as he erroneously assumed. For a drop where $a_0 \approx 0.35$ cm, $p_{ic} \approx 112$ dyn cm^{-2} based on the maximum internal speed. According to McDonald (1954, Fig. 4), the quantity $(p_e-p_\infty)-p_{ic}$ at the position of the maximum internal speed but just outside the drop is ~ 450 dyn cm^{-2}. Thus, p_e-p_∞ at this position becomes ~ 562 dyn cm^{-2}. This makes p_{ic} about 20% of p_e-p_∞, which is considerably less than the percentage estimated by Foote, who erroneously assumed that the maximum internal circulation velocity occurs for all drop sizes at the drop equator, but still large enough that the contribution to the internal pressure by the internal circulation can by no means be neglected. Unfortunately, a quantitative evaluation of p_{ic} over the whole Reynolds number interval in question is not possible at the moment since the only estimate of this quantity is that given by Foote, which is at best applicable to very large drops with large internal Reynolds numbers.

A new avenue of approaching the problem was found when we compared the distribution of $[p_e(\theta)-p_\infty] - p_{ic}(\theta)$ around a drop, measured by McDonald, with the distribution of $p_e(\theta)-p_\infty$ around a rigid sphere. For this comparison McDonald's coordinate system was changed from (p_e-p_∞) vs z to our coordinate system $(p_e-p_\infty)/(\frac{1}{2}\rho_a V_\infty^2)$ vs θ. A further slight adjustment of McDonald's pressure values was necessary since he based the values for the stagnation pressure on older data for the terminal velocity of water drops in air. This correction caused a rise of each pressure distribution by a small constant factor. The comparison showed that for $a_0 \leqslant 0.25$ cm the aerodynamic pressure distribution around a rigid sphere well approximates McDonald's quantity $(p_e-p_\infty)-p_{ic}$ around a drop. For drops of $a_0 > 0.25$ cm the characteristic pressure minimum becomes progressively deeper until for $a_0 = 0.35$ cm the minimum of $(p_e-p_\infty)-p_{ic}$ at a drop is $\sim 15\%$ lower than the minimum of p_e-p_∞ at a rigid sphere. The good agreement of these two quantities motivated us to replace in Eq. (4) the term $\{[p_e(\theta)-p_\infty]-p_{ic}(\theta)\}$ for a deformed water drop in air by the term $[p_e(\theta)-p_\infty]$ for a rigid sphere and to compute the drop shape on the basis of the modified equation. The pressure distribution enters into the deformation through its cosine series coefficients q_n which are defined as

$$[p_e(\theta)-p_\infty]/(\tfrac{1}{2}\rho_a V_\infty^2) = \sum_{n=0}^{\infty} q_n \cos n\theta, \qquad (7)$$

and which determine the deformation coefficients through (4). It turns out that the entire percentage error in the pressure distribution minimum does not become the error in the deformation of the drop. Our results indicate that the deformation percentage error is only about half of the error in the pressure distribution minimum.

Considering the discussion above the pressure balance equation can now be written as

$$J(\theta) = N_{\mathrm{Bo}}(r_0' + r' \cos\theta) - N_{\mathrm{we}} \sum_{n=0}^{\infty} q_n \cos n\theta + K, \quad (8)$$

where

$$J(\theta)=2+\sum_{n=0}^{\infty}(n^2-2)c_n\cos n\theta + \sum_{n=0}^{\infty} nc_n \sum_{m=1}^{n}\cos(n-2m)\theta,$$

$N_{\mathrm{Bo}}=a_0^2\rho_w g/\sigma$ is the Bond number, $N_{\mathrm{We}}=\frac{1}{2}\rho_a V_\infty^2/\sigma$ the Weber number, and

$$\left.\begin{aligned} K&=a_0[p_i(\theta=\pi)-p_\infty]/\sigma \\ r_0'&=r_0/a_0=1+\sum_{n=0}^{\infty}c_n\cos n\pi \\ r'&=r/a_0=1+\sum_{n=0}^{\infty}c_n\cos n\theta \end{aligned}\right\}. \tag{8a}$$

For numerical solution (8) was expanded as

$$\begin{aligned} -N_{\mathrm{Bo}}&\left\{1+\sum_{n=0}^{\infty}c_n\cos n\pi+\cos\theta \right. \\ &\left.+\tfrac{1}{2}\sum_{n=0}^{\infty}c_n[\cos(n+1)\theta+\cos(n-1)\theta]\right\} \\ &+\left[2+\sum_{n=0}^{\infty}(n^2-2)c_n\cos n\theta \right. \\ &\left.+\sum_{n=0}^{\infty}nc_n\sum_{m=1}^{n}\cos(n-2m)\theta\right] \\ &=-N_{\mathrm{We}}\sum_{n=0}^{\infty}q_n\cos n\theta+K. \end{aligned} \tag{9}$$

The deformation of the drop is constrained by the conservation of the volume of the drop, which drop is given by

$$V=\int_0^{\pi}\tfrac{2}{3}r^3\pi\sin\theta d\theta. \tag{10}$$

Introducing Eqs. (5) into (10), and assuming that the term in the parentheses of (5) is near 1, we can write approximately

$$V=(4\pi a_0^3/3)+2\pi a_0^3\int_0^{\pi}\sum_{n=0}^{\infty}c_n\cos n\theta\sin\theta d\theta. \tag{11}$$

The condition for volume conservation is therefore

$$\int_0^{\pi}\sum_{n=0}^{\infty}c_n\cos n\theta\sin\theta d\theta=0. \tag{12}$$

Extracting the c_0 term from (12), we have

$$\int_0^{\pi}c_0\sin\theta d\theta+\int_0^{\pi}\sum_{n=1}^{\infty}c_n\cos n\theta\sin\theta d\theta=0,$$

or

$$c_0=\tfrac{1}{2}\int_0^{\pi}\sum_{n=1}^{\infty}c_n\cos n\theta\sin\theta d\theta. \tag{13}$$

It can readily be shown that this summation can be transformed into

$$c_0=\tfrac{1}{2}\sum_{n=1}^{\infty}c_{2n}\int_0^{\pi}\cos 2n\theta\sin\theta d\theta, \tag{14}$$

which may further be transformed into

$$c_0=\sum_{n=1}^{\infty}c_{2n}/(4n^2-1). \tag{15}$$

Eq. (15) shows that c_0 can be found when the deformation coefficients $c_2, c_4, \cdots, c_{2n}$ are found. Thus, the constant terms, including K, in Eq. (9) need not be evaluated. Also, the coefficient c_1 acts only through the $\cos 1\theta$ term, which is not a deformation term, but a vertical displacement term. Without loss of generality, we set $c_1\equiv 0$. In our computations we truncated (9) at $n=9$. Table 3, applicable to drops of $a_0=0.40$ cm, shows that beyond the first few terms the deformation coefficients indeed are small, and are merely smoothing parameters. Hence, our truncation at c_9 does not cause any noticeable error. Our computations then involved the equations within the box of Table 1 from which $c_2\cdots c_9$ were determined. The coefficient c_0 could then be found from (15). For our computations we set $\sigma=72.75$ ergs cm^{-2}, $\rho_a=1.188\times10^{-3}$ gm cm^{-3}, $\nu_a=0.153$ cm^2 sec^{-1} and $g=980$ cm sec^{-2}, all applying at 20C. Beard and Pruppacher (1969) and Gunn and Kinzer (1949) were used to find V_∞ for various drops. For drop sizes with $N_{\mathrm{Re}}\geqslant 1000$ the pressure distribution coefficients q_0 through q_9 were obtained by a Fourier series fit to the pressure distribution given by Fage (1937). For smaller Reynolds numbers similar fits were made to the results of LeClair *et al.* (1970). The values for the deformation coefficients, placed into (8a), yielded values of r'. Computations were performed on an IBM 360/91 electronic computer.

3. Results

The deformation coefficients computed for 15 drop sizes selected for this study are listed in Table 2. In Table 3 the relative magnitude of these coefficients is given for a drop of $a_0=0.4$ cm. As mentioned above, terms of order higher than $n=9$ in Eq. (9) can safely be neglected. In Fig. 2 the shape of 9 selected drops is graphically displayed by a plot of r' vs θ in a meridional plane through the drop center on polar diagrams. The corresponding silhouette shape of a drop (which is the

TABLE 1. Set of equations which describe the shape of a drop in terms of the deformation coefficients and pressure coefficients.

$-N_{Bo}-N_{Bo}[\sum_{n=0}^{9}(-1)^n c_n]+2-2c_0$	$-\frac{1}{2}N_{Bo}c_1$	$+2c_2$	$+0$	$+4c_4$	$+0$	$+6c_6$	$+0$	$+8c_8$	$+0$	$\equiv -N_{We}q_0$
$-N_{Bo}-N_{Bo}c_0$	$+0$	$-\frac{1}{2}N_{Bo}c_2$	$+6c_3$	$+0$	$+10c_5$	$+0$	$+14c_7$	$+0$	$+18c_9$	$\equiv -N_{We}q_1$
	$-\frac{1}{2}N_{Bo}c_1$	$+4c_2$	$-\frac{1}{2}N_{Bo}c_3$	$+8c_4$	$+0$	$+12c_6$	$+0$	$+16c_8$	$+0$	$\equiv -N_{We}q_2$
		$-\frac{1}{2}N_{Bo}c_2$	$+10c_3$	$-\frac{1}{2}N_{Bo}c_4$	$+10c_5$	$+0$	$+14c_7$	$+0$	$+18c_9$	$\equiv -N_{We}q_3$
			$-\frac{1}{2}N_{Bo}c_3$	$+18c_4$	$-\frac{1}{2}N_{Bo}c_5$	$+12c_6$	$+0$	$+16c_8$	$+0$	$\equiv -N_{We}q_4$
				$-\frac{1}{2}N_{Bo}c_4$	$+28c_5$	$-\frac{1}{2}N_{Bo}c_6$	$+14c_7$	$+0$	$+18c_9$	$\equiv -N_{We}q_5$
					$-\frac{1}{2}N_{Bo}c_5$	$+40c_6$	$-\frac{1}{2}N_{Bo}c_7$	$+16c_8$	$+0$	$\equiv -N_{We}q_6$
						$-\frac{1}{2}N_{Bo}c_6$	$+54c_7$	$-\frac{1}{2}N_{Bo}c_8$	$+18c_9$	$\equiv -N_{We}q_7$
							$-\frac{1}{2}N_{Bo}c_7$	$+70c_8$	$-\frac{1}{2}N_{Bo}c_9$	$\equiv -N_{We}q_8$
								$-\frac{1}{2}N_{Bo}c_8$	$+88c_9$	$\equiv -N_{We}q_9$

shape as it appears to an observer looking at the drop from the side) can be obtained by connecting the lowest points of the shape outlines in Fig. 2 with a straight line. From the computed shape of each drop the deformation a/b, where a is the distance between the top and the silhouette base of the drop and b is the greatest width of the drop (see Fig. 1), was determined and is listed in Table 4 as a function of a_0, N_{Re}, N_{Bo} and N_{We}. The variation of the computed values for a/b with a_0 is plotted in Fig. 3 and is compared with the deformations experimentally found from the photograph of drops floating freely in the air stream of a wind tunnel (Pruppacher and Beard, 1970; and present values). For comparison, the results found from an evaluation of Imai's (1950) theory is also given in Fig. 3.

From Figs. 2 and 3 it is seen that the drop shapes and deformations predicted by our model agree well with those experimentally observed except for the very largest drops under consideration, whose deformation we slightly underestimated. Our computations indicate further that the drop deformation a/b asymptotically approaches 1.0 as a_0 approaches zero. However, for practical purposes, drops of $a_0 \lesssim 170\,\mu$ can, with negligible error, be considered spherical. Drops of radii 170–500 μ are deformed into oblate spheroids. Their deformations increase only slightly with increasing a_0. Drops of $a_0 \gtrsim 500\,\mu$ become progressively deformed into asymmetric spheroids. A flat base occurs when $a_0 \approx 0.2$ cm. Drops of $a_0 \gtrsim 0.2$ cm develop concave depressions in the drop bases which rapidly deepen as a_0 increases. An excellent photograph of a drop which shows a well developed concave depression in the drop base is given by Koenig (1965, Fig. 1a).

4. Discussion of the drop shape in terms of drop breakup

Our model presented in the foregoing section is based on equilibrium considerations. Consequently, it is not capable of predicting the size at which a drop becomes hydrodynamically unstable and breaks up. Experiments carried out by Fournier d'Albe and Hidayetulla (1955) with drops falling in a long column of quiet air, by Blanchard (1948, 1950, 1962) and by Beard and Pruppacher (1969) with drops suspended in very low turbulence wind tunnels, have shown that the largest drop which can fall without breaking, even in completely quiet air, is $a_0 \approx 0.45$ cm. We may ask what the exact mechanism is which brings about a force imbalance on the drop. Numerous mechanisms of drop breakup have been suggested in literature. One mechanism which could be used for explaining the breakup of water drops in air was proposed by Komabayasi *et al.* (1964). These investigators assumed that Lamb's theory (1932) of infinite, plane-parallel surface waves (capillary-gravity waves) may be applied to the top and bottom surface of a drop, and suggested that drop breakup is related to the condition for instability of such waves. The square

TABLE 2. Computed deformation coefficients as a function of drop size.

	Deformation coefficients, $C\times10^5$								
a_0(cm)	c_0	c_2	c_3	c_4	c_5	c_6	c_7	c_8	c_9
0.01711	−12	−36	−3	0	0	0	0	0	0
0.03505	−69	−208	−27	0	1	0	0	0	0
0.0433	−181	−543	−97	−3	5	−2	0	0	0
0.0532	−314	−939	−189	−12	10	−1	0	−1	0
0.062	−447	−1334	−300	−27	17	−2	1	−1	1
0.11	−1431	−4259	−1105	−173	62	25	3	−12	−4
0.14	−2344	−6977	−1843	−288	101	42	5	−19	−7
0.15	−2670	−7948	−2114	−330	115	48	5	−22	−8
0.18	−3659	−10889	−2963	−462	156	65	8	−30	−11
0.20	−4296	−12783	−3539	−551	182	77	9	−35	−13
0.25	−5734	−17053	−4959	−775	237	102	12	−47	−18
0.29	−6822	−20280	−6166	−971	274	122	14	−55	−21
0.30	−7089	−21070	−6482	−1023	283	127	15	−57	−22
0.35	−8380	−24888	−8151	−1310	318	149	18	−67	−25
0.40	−9763	−28966	−10143	−1677	346	173	21	−76	−29

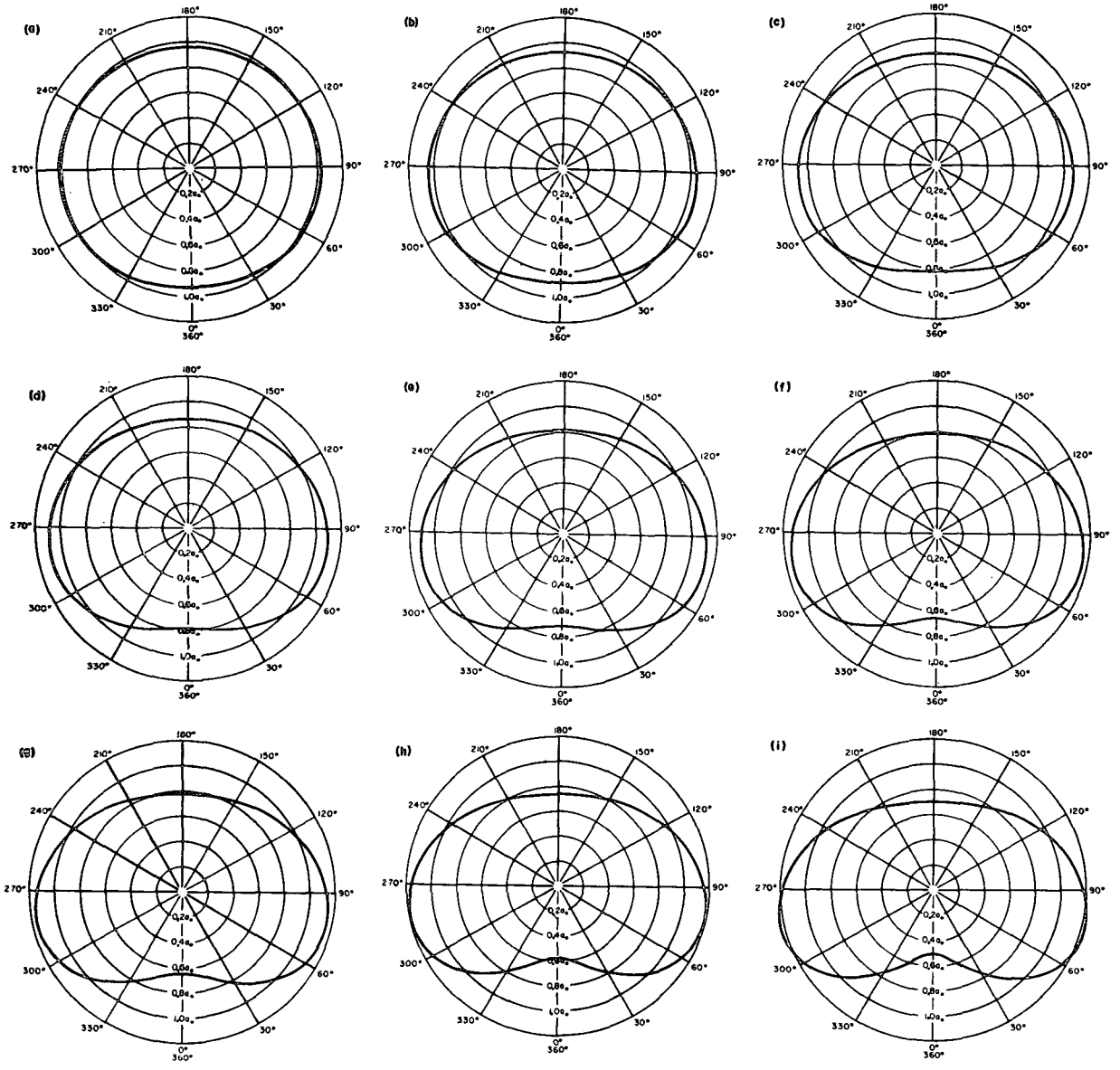

FIG. 2. Computed shape of selected drops: a_0=0.11, 0.14, 0.18, 0.20, 0.25, 0.29, 0.30, 0.35, 0.40 cm for (a)–(g), respectively.

TABLE 3. Relative magnitude of the deformation coefficients for $a_0=0.4$ cm.

n	2	3	4	5	6	7	8	9
c_n/c_2	1.000	0.350	0.058	0.012	0.006	0.0007	0.0026	0.0010

TABLE 4. Variation of the drop deformation as a function of drop size, Reynolds number, Weber number and Bond number.

a_0 (cm)	V_∞ (cm sec^{-1})	N_{Re}	N_{We}	N_{Bo}	a/b
0.0170	133	30	0.003	0.004	0.9993
0.0305	249	100	0.016	0.013	0.9959
0.0433	351	200	0.044	0.025	0.9892
0.0532	424	300	0.078	0.038	0.9813
0.0620	478	400	0.116	0.052	0.9735
0.11	690	1013	0.428	0.163	0.916
0.14	782	1430	0.700	0.264	0.865
0.15	806	1613	0.796	0.303	0.847
0.18	860	2066	1.087	0.436	0.795
0.20	883	2357	1.273	0.539	0.762
0.25	909	3033	1.687	0.842	0.701
0.29	917	3549	1.991	1.133	0.664
0.30	918	3600	2.060	1.211	0.655
0.35	918	4288	2.408	1.650	0.621
0.40	919	4900	2.758	2.155	0.583

of the phase speed C_1 at a plane fluid interphase, where the upper fluid is air and the lower fluid is water, and the square of the phase speed C_2 at an interphase with water as the upper fluid and air as the lower fluid are plotted as a function of the wavelength λ in Fig. 4. We shall now interpret this figure in terms of waves on the top and bottom surface of a water drop falling in air and combine the interpretation with our results on the drop shape. It is seen from Fig. 4 that the waves on the top surface of a drop are stable for all wavelengths. However, the waves on the bottom surface of the drop are unstable and will amplify if $\lambda \gtrsim \lambda_c$, where $\lambda_c=1.71$ cm. This suggests that the breakup of a drop always will proceed from the bottom of a drop rather than the top, which is in agreement with most observations. For the development of a standing wave on the bottom surface of a drop, the width d of the drop base has to fulfill the requirement $d=n(\lambda/2)$, where n is an integer. For the fundamental mode of a standing wave $n=1$. Thus, if $d \gtrsim \lambda_c/2=0.855$ cm, a standing wave on the bottom surface of a drop will amplify and cause the drop to break up. In order to interpret this result we extended our drop shape computations to $a_0=0.45$ and 0.50 cm and measured the base width of the computed drop shapes. We found that $d \approx 0.855$ cm for $0.45 \lesssim a_0 \lesssim 0.50$ cm. Drops of this size have a pronounced concave depression in the base. If we assume that this depression represents a wave-like disturbance which is composed of an infinite number of simple waves, one of which has a wavelength equal to λ_c, we are led to the conclusion that drops of a_0 larger than the abovementioned critical size will be hydrodynamically unstable and break up even if they would fall in completely calm air. However, the above agreement between Lamb's theory and our theoretical results is not well justified. Drops with $a_0>0.35$ cm observed in our wind tunnel have somewhat greater deformations than our theory predicts. Also, drops with $a_0 \approx 0.45$ cm observed in the wind tunnel have a base width $d \approx 1.05$ cm which is larger than Lamb's theory predicts as critical width. We feel that a more rigorous treatment of the surface waves on the bottom of the drops would yield better results.

The other end of the spectrum of drops liable to break up was investigated by Blanchard (1948, 1950, 1962), Komabayasi *et al.* (1964) and Cotton and Gokhale (1967). These investigators found that drops of $a_0 \lesssim 0.20$ cm are very resistant to breakup even if the air in which they fell was very turbulent. Comparing this result with the results of our computations, it is interest-

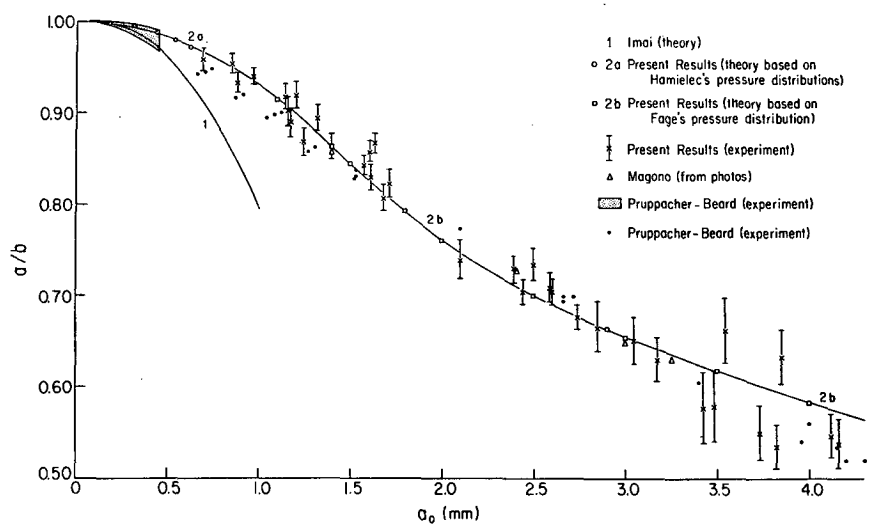

FIG. 3. Variation of drop deformation with drop size: comparison of theory and experiment.

ing to note that according to our findings drops of $a_0<0.20$ cm have no concave depression in the drop base. This suggests that the concave depression in the drop base is a necessary requirement for drop breakup. However, this requirement, even though necessary, seems to be a sufficient one only for drops of a_0 larger than the critical size. Drops of $0.20\lesssim a_0\lesssim 0.45$ cm will break up only if some additional conditions are fulfilled. Unfortunately, these are still not sufficiently understood. One such condition seems to be the setting up of oscillations in the drop (Blanchard, 1948, 1950, 1962; Komabayasi *et al.*; Cotton and Gokhale).

Oscillations could conceivably be induced into a falling drop by means of the periodic detachment of eddies from the rear of the drop which through a resonance effect excite the drop at the natural frequencies of oscillation. In Fig. 5 the natural frequencies of oscillation of a liquid sphere, given in Lamb (1932) by the relation

$$f=[n(n-1)(n+2)\sigma/(4\pi^2\rho_w a_0^3)]^{\frac{1}{2}}, \qquad (16)$$

are plotted as a function of a_0. The oscillation frequency of the wake and the shedding frequency of eddies from the rear of a rigid sphere deduced from the experimental result of Möller (1938) are also plotted in Fig. 5. It is seen from Fig. 5 that resonance between the natural drop vibration and the eddy detachment from the rear of a drop can hardly be considered a mechanism which is responsible for drop breakup. Despite the numerous resonance frequencies in the drop size interval $0.05\lesssim a_0\lesssim 0.2$ cm, drops of these sizes and smaller rarely break up. However, the first resonance mode at $a_0\approx 480\,\mu$ may cause the transversal shift typical for drops of $a_0\gtrsim 500\,\mu$ falling in air (Gunn, 1949).

Alternatively, oscillations can be set up in a falling drop by means of resonance between natural drop vibration and the turbulence of the air in which the drop is falling. While drop breakup by such a resonance mechanism may be conceivable under laboratory conditions (Blanchard, 1948, 1950, 1962; Komabayasi, *et al.*; Cotton and Gokhale), it is questionable whether it is operating in atmospheric clouds. During a storm, the size of the raindrops which strike the ground usually varies over a wide range. However, the largest drops from warm clouds rarely have a size $a_0>0.25$–0.30 cm (Blanchard, 1962). According to our drop shape computations, the concave depression in drops of such sizes is not yet well developed and the width of the drop base is considerably less than the critical one. Therefore, rather strong oscillations would have to be set up if such drops should break up. As did Blanchard (1962) and McDonald (1959), we question whether at cloud level the turbulence both is fine grained enough for inducing a resonance effect and has sufficient energy to cause the oscillations necessary for drop breakup. Therefore, it seems to us rather unlikely that in atmospheric clouds drop breakup is caused by the "bag breakup

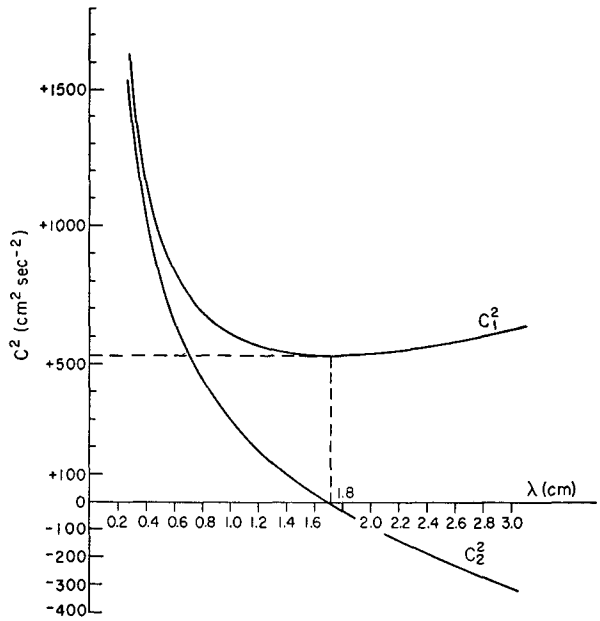

FIG. 4. Variation of the square of the phase velocity of surface capillary-gravity waves with wavelength (after Komabayasi *et al.*, 1964).

mechanism" involving single drops whose concave depression develops into a rapidly expanding bubble (Blanchard, 1948, 1950; Magarvey and Taylor, 1956; Mathews and Mason 1964; Koenig, 1965). Rather, we suspect that in atmospheric clouds in which drops grow predominantly by collision and coalescence the breakup of drops is the result of drop collisions. Following the collision of two drops an oscillating system is formed which is highly unstable during the initial moments of

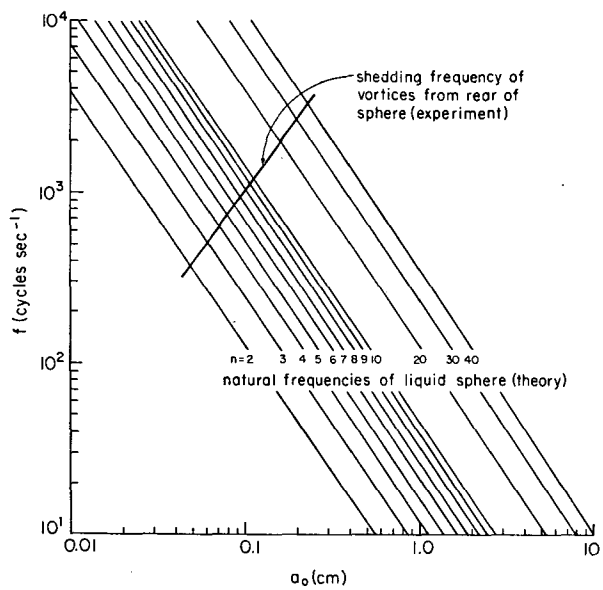

FIG. 5. Variation of the natural oscillation frequence of a liquid water sphere and variation of the shedding frequency of eddies from a rigid water sphere in air with size of sphere.

coalescence. Parallel to our discussion on the breakup of large, single drops, we may consider this oscillating system as one with a wave-like disturbance in the base. This disturbance will amplify whenever the base of the oscillating system reaches in its largest elongation a width $\geqslant 1.05$ cm. Under these conditions the system will disrupt into fragment drops. Our drop shape computations indicate that a dumbbell system of two drops of $a_0 = 0.25$ cm, passing each other on a critical collision trajectory, will have a base width $d = 1.05$ cm at the moment of collision and consequently will disrupt, as observed by Blanchard (1948, 1950, 1962) and by Cotton and Gokhale. If the drops collide more directly the oscillations may lead to a bag-breakup.

It is hoped that the results and discussion presented in this paper stimulate further work which is very much needed.

Acknowledgments. The authors are indebted to the National Science Foundation (Grants GA-759 and GA-18531) for supporting the research reported in this paper.

REFERENCES

Batchelor, G. K., 1967: *An Introduction to Fluid Dynamics.* Cambridge University Press, 613 pp.

Beard, K., and H. Pruppacher, 1969: A determination of the terminal velocity and drag of small water drops by means of a wind tunnel. *J. Atmos. Sci.*, **26**, 1066–1072.

Best, A. C., 1947: The shape of raindrops and mode of disintegration of large drops. Air Ministry, Great Britain, Meteor. Res. Comm., Rept. M.R.P. 330.

Blanchard, D. C., 1948: Observations on the behavior of water drops at terminal velocity in air. Gen. Electric Res. Lab., Occasional Rept. No. 7, Project Cirrus, 13 pp.

——, 1950: The behavior of water drops at terminal velocity. *Trans. Amer. Geophys. Union*, **31**, 836–842.

——, 1955: Comments on "The shape of water drops falling in stagnant air." *J. Meteor.*, **12**, 91–93.

——, 1962: Comments on the breakup of raindrops. *J. Atmos. Sci.*, **19**, 119–120.

Cotton, W. R., and N. R. Gokhale, 1967: Collision, coalescence and breakup of large water drops in a vertical wind tunnel. *J. Geophys. Res.*, **72**, 4041–4049.

Eichelbrenner, E. A., and R. Michel, 1957: Vergleich von theoretischen Ansatzen zur Bestimmung des Umschlags laminar-turbulent. *Proc. Symp. Grenzschichtforschung*, Freiburg/BR., 161–172.

Fage, A., 1937: Experiments on a sphere at critical Reynolds numbers. Aero. Res. Comm., England, Rept. and Memo. No. 1766, 20 pp.

Flachsbart, O., 1927: Untersuchugen uber den Luftwiderstand von Kugeln. *Phys. Z.*, **28**, 461–469.

Foote, G. B., 1969: On the internal circulation and shape of large raindrops. *J. Atmos. Sci.*, **26**, 179–181.

Fournier d'Albe, E. M., and M. S. Hidayetulla, 1955: The break-up of large water drops falling at terminal velocity in free air. *Quart. J. Roy. Meteor. Soc.*, **81**, 610–613.

Garner, F. H., and J. J. Lane, 1959: Mass transfer to drops of liquid suspended in a gas stream. *Trans. Instr. Chem. Eng.*, **37**, 167–172.

Gunn, R., 1949: Mechanical resonance in freely falling raindrops. *J. Geophys. Res.*, **54**, 383–385.

——, and G. D. Kinzer, 1949: The terminal velocity of fall for water drops in stagnant air. *J. Meteor.*, **6**, 243–248.

Imai, I., 1950: On the velocity of falling raindrops. *Geophys. Mag. Tokyo*, **21**, 244–249.

Jones, D. M., 1959: The shape of raindrops. *J. Meteor.*, **16**, 504–510.

Koenig, R., 1965: Drop freezing through drop breakup. *J. Atmos. Sci.*, **22**, 448–451.

Komabayasi, M., T. Gonda and K. Isono, 1964: Lifetime of water drops before breaking and size distribution of fragment drops. *J. Meteor. Soc. Japan, Ser. 2*, **42**, 330–340.

Kumai, M., and K. Itagaki, 1954: Shape and fall velocity of rain drops. *J. Meteor. Soc. Japan*, **32**, 1–18.

Lamb, H., 1932: *Hydrodynamics*, 6th ed. New York, Dover, 738 pp.

Landau, L. D., and E. M. Lifshitz, 1959: *Fluid Mechanics.* London, Pergamon Press, 536 pp. (see section on Capillarity, 230–244).

Langmuir, I., 1948: Production of rain by a chain reaction in cumulus clouds at temperatures above freezing. *J. Meteor.*, **5**, 175–192.

Le Clair, B. A. Hamielec and H. R. Pruppacher, 1970: A numerical study of the drag on a sphere at low and intermediate Reynolds numbers. *J. Atmos. Sci.*, **27**, 308–315.

Lenard, P., 1904: Ueber Regen. *Meteor. Z.*, **21**, 249–260.

Magarvey, R. H., and B. W. Taylor, 1956: Free fall breakup of large drops. *J. Appl. Phys.*, **27**, 1129–1135.

Magono, C., 1954: On the shape of water drops falling in stagnant air. *J. Meteor.*, **11**, 77–79.

Maruhn, K., 1940: Druckverteilung auf den gleich formig-geradlinig bewegten 3-achsigen Ellipsoidkorper. *Deut. Versuchsanstalt Luftfahrtforschung*, Ber. No. 1174, 20 pp.

Mathews, J. B., and B. J. Mason, 1964: Electrification produced by rupture of large water drops in an electric field. *Quart. J. Roy. Meteor. Soc.*, **90**, 275–286.

McDonald, J. E., 1954: The shape and aerodynamics of large raindrops. *J. Meteor.*, **11**, 478–494.

——, 1959: Comments on behavior of water drops at terminal velocity in air. *Trans. Amer. Geophys. Union*, **32**, 775–776.

Möller, W., 1938: Experimentelly Untersuchungen zur Hydrodynamik der Kugel. *Phys. Z.*, **39**, 57–80.

Pruppacher, H. R., and K. Beard, 1970: A wind tunnel investigation of the internal circulation and shape of water drops falling at terminal velocity in air. *Quart. J. Roy. Meteor. Soc.*, **96**, 247–256.

Savic, P., 1953: Circulation and distortion of liquid drops falling through a viscous medium. Natl. Res. Council, Canada, Rept. NRC-MT-22, 50 pp.

Spilhaus, A. F., 1948: Raindrop size, shape and falling speed. *J. Meteor.*, **5**, 108–110.

Taylor, T. D., and A. Acrivos, 1964: The deformation and drag on a falling viscous drop at low Reynolds numbers. *J. Fluid Mech.*, **18**, 446–470.